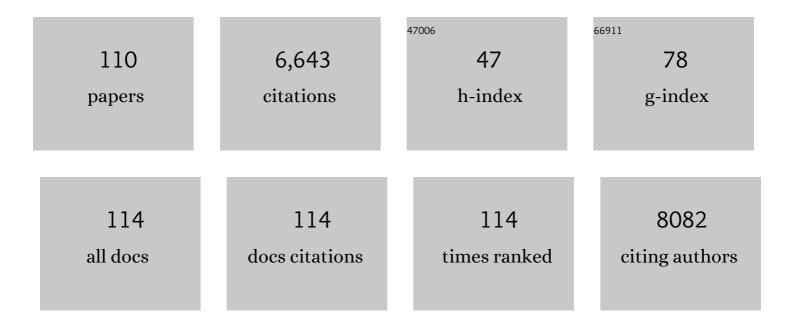
## List of Publications by Year in descending order

Source: https://exaly.com/author-pdf/7702749/publications.pdf Version: 2024-02-01



#	Article	IF	CITATIONS
1	Engineering of ZnCo-layered double hydroxide nanowalls toward high-efficiency electrochemical water oxidation. Journal of Materials Chemistry A, 2014, 2, 13250.	10.3	323
2	Surface Modification of Halloysite Nanotubes with Dopamine for Enzyme Immobilization. ACS Applied Materials & Interfaces, 2013, 5, 10559-10564.	8.0	300
3	Hierarchical hollow nanotubes of NiFeV-layered double hydroxides@CoVP heterostructures towards efficient, pH-universal electrocatalytical nitrogen reduction reaction to ammonia. Applied Catalysis B: Environmental, 2020, 265, 118559.	20.2	252
4	Recent advances in magnesium/lithium separation and lithium extraction technologies from salt lake brine. Separation and Purification Technology, 2021, 256, 117807.	7.9	229
5	Highly Enhanced Photoelectrochemical Water Oxidation Efficiency Based on Triadic Quantum Dot/Layered Double Hydroxide/BiVO <sub>4</sub> Photoanodes. ACS Applied Materials & Interfaces, 2016, 8, 19446-19455.	8.0	227
6	Enhanced photoelectrochemical water oxidation on a BiVO <sub>4</sub> photoanode modified with multi-functional layered double hydroxide nanowalls. Journal of Materials Chemistry A, 2015, 3, 17977-17982.	10.3	201
7	Facile Synthesis and Characterization of Cobalt Ferrite Nanocrystals via a Simple Reductionâ^'Oxidation Route. Journal of Physical Chemistry C, 2008, 112, 18459-18466.	3.1	184
8	Fabricating of Fe2O3/BiVO4 heterojunction based photoanode modified with NiFe-LDH nanosheets for efficient solar water splitting. Chemical Engineering Journal, 2018, 350, 148-156.	12.7	162
9	Selective Activation of Benzyl Alcohol Coupled with Photoelectrochemical Water Oxidation via a Radical Relay Strategy. ACS Catalysis, 2020, 10, 4906-4913.	11.2	154
10	Layered Double Hydroxides as Catalytic Materials: Recent Development. Catalysis Surveys From Asia, 2008, 12, 253-265.	2.6	152
11	Facile synthesis and novel electrocatalytic performance of nanostructured Ni–Al layered double hydroxide/carbon nanotube composites. Journal of Materials Chemistry, 2010, 20, 3944.	6.7	140
12	Self-generated Template Pathway to High-Surface-Area Zinc Aluminate Spinel with Mesopore Network from a Single-Source Inorganic Precursor. Chemistry of Materials, 2006, 18, 5852-5859.	6.7	130
13	Strong Electronic Coupling and Ultrafast Electron Transfer between PbS Quantum Dots and TiO <sub>2</sub> Nanocrystalline Films. Nano Letters, 2012, 12, 303-309.	9.1	130
14	In situ probe of photocarrier dynamics in water-splitting hematite (α-Fe2O3) electrodes. Energy and Environmental Science, 2012, 5, 8923.	30.8	121
15	Ternary MgO/ZnO/In2O3 heterostructured photocatalysts derived from a layered precursor and visible-light-induced photocatalytic activity. Chemical Engineering Journal, 2013, 221, 222-229.	12.7	121
16	Space-Confined Earth-Abundant Bifunctional Electrocatalyst for High-Efficiency Water Splitting. ACS Applied Materials & Interfaces, 2017, 9, 36762-36771.	8.0	114
17	Lattice-Confined Sn (IV/II) Stabilizing Raft-Like Pt Clusters: High Selectivity and Durability in Propane Dehydrogenation. ACS Catalysis, 2017, 7, 6973-6978.	11.2	109
18	Electron Transfer Dynamics in Semiconductor–Chromophore–Polyoxometalate Catalyst Photoanodes. Journal of Physical Chemistry C, 2013, 117, 918-926.	3.1	108

#	Article	IF	CITATIONS
19	Single-Crystalline ZnGa <sub>2</sub> O <sub>4</sub> Spinel Phosphor via a Single-Source Inorganic Precursor Route. Inorganic Chemistry, 2008, 47, 1361-1369.	4.0	99
20	An Integrating Photoanode of WO <sub>3</sub> /Fe <sub>2</sub> O <sub>3</sub> Heterojunction Decorated with NiFe-LDH to Improve PEC Water Splitting Efficiency. ACS Sustainable Chemistry and Engineering, 2018, 6, 12906-12913.	6.7	96
21	Photoelectrochemical Water Oxidation Efficiency of a Core/Shell Array Photoanode Enhanced by a Dual Suppression Strategy. ChemSusChem, 2015, 8, 1568-1576.	6.8	95
22	Co-based catalysts from Co/Fe/Al layered double hydroxides for preparation of carbon nanotubes. Applied Clay Science, 2009, 42, 405-409.	5.2	89
23	Ultrafine MnO 2 nanoparticles decorated on graphene oxide as a highly efficient and recyclable catalyst for aerobic oxidation of benzyl alcohol. Journal of Colloid and Interface Science, 2016, 483, 26-33.	9.4	83
24	Surface functionalization of Co3O4 hollow spheres with ZnO nanoparticles for modulating sensing properties of formaldehyde. Sensors and Actuators B: Chemical, 2017, 245, 359-368.	7.8	82
25	Facile Synthesis and Catalytic Properties of Nickel-Based Mixed-Metal Oxides with Mesopore Networks from a Novel Hybrid Composite Precursor. Chemistry of Materials, 2008, 20, 1173-1182.	6.7	78
26	Long lived charge separation in iridium(iii)-photosensitized polyoxometalates: synthesis, photophysical and computational studies of organometallic–redox tunable oxide assemblies. Chemical Science, 2013, 4, 1737.	7.4	75
27	Solarâ€Driven H <sub>2</sub> O <sub>2</sub> Generation From H <sub>2</sub> O and O <sub>2</sub> Using Earthâ€Abundant Mixedâ€Metal Oxide@Carbon Nitride Photocatalysts. ChemSusChem, 2016, 9, 2470-2479.	6.8	75
28	Selective Activation of C–OH, C–O–C, or Câ•C in Furfuryl Alcohol by Engineered Pt Sites Supported on Layered Double Oxides. ACS Catalysis, 2020, 10, 8032-8041.	11.2	73
29	Natural Nanotube-Based Biomimetic Porous Microspheres for Significantly Enhanced Biomolecule Immobilization. ACS Sustainable Chemistry and Engineering, 2014, 2, 396-403.	6.7	68
30	Highly efficient extraction of lithium from salt lake brine by LiAl-layered double hydroxides as lithium-ion-selective capturing material. Journal of Energy Chemistry, 2019, 34, 80-87.	12.9	68
31	Water splitting with polyoxometalate-treated photoanodes: enhancing performance through sensitizer design. Chemical Science, 2015, 6, 5531-5543.	7.4	67
32	Enhancing Photoelectrochemical Water Oxidation Efficiency of BiVO <sub>4</sub> Photoanodes by a Hybrid Structure of Layered Double Hydroxide and Graphene. Industrial & Engineering Chemistry Research, 2017, 56, 10711-10719.	3.7	67
33	Facile Sodium Alginate Assisted Assembly of Niâ^'Al Layered Double Hydroxide Nanostructures. Industrial & Engineering Chemistry Research, 2010, 49, 2759-2767.	3.7	61
34	Assembly of Ruthenium-Based Complex into Metal–Organic Framework with Tunable Area-Selected Luminescence and Enhanced Photon-to-Electron Conversion Efficiency. Journal of Physical Chemistry C, 2014, 118, 25365-25373.	3.1	61
35	Energy-level dependent H 2 O 2 production on metal-free, carbon-content tunable carbon nitride photocatalysts. Journal of Energy Chemistry, 2018, 27, 343-350.	12.9	60
36	Preparation of ternary Pd/CeO2-nitrogen doped graphene composites as recyclable catalysts for solvent-free aerobic oxidation of benzyl alcohol. Applied Surface Science, 2019, 471, 852-861.	6.1	60

#	Article	IF	CITATIONS
37	Research Progress in Organic Synthesis by Means of Photoelectrocatalysis. Chemical Record, 2021, 21, 841-857.	5.8	60
38	A mild solution chemistry method to synthesize hydrotalcite-supported platinum nanocrystals for selective hydrogenation of cinnamaldehyde in neat water. Catalysis Science and Technology, 2013, 3, 2819.	4.1	57
39	Increasing the Activity and Selectivity of TiO <sub>2</sub> -Supported Au Catalysts for Renewable Hydrogen Generation from Ethanol Photoreforming by Engineering Ti <sup>3+</sup> Defects. ACS Sustainable Chemistry and Engineering, 2019, 7, 13856-13864.	6.7	57
40	An integrated membrane process for preparation of lithium hydroxide from high Mg/Li ratio salt lake brine. Desalination, 2020, 493, 114620.	8.2	56
41	Ultrafine PtCo Alloy Nanoclusters Confined in N-Doped Mesoporous Carbon Spheres for Efficient Ammonia Borane Hydrolysis. ACS Sustainable Chemistry and Engineering, 2021, 9, 822-832.	6.7	54
42	Recent Advances in Heterogeneous Photoâ€Driven Oxidation of Organic Molecules by Reactive Oxygen Species. ChemSusChem, 2020, 13, 5173-5184.	6.8	53
43	Single-Source Precursor to Complex Metal Oxide Monoliths with Tunable Microstructures and Properties: The Case of Mg-Containing Materials. Chemistry of Materials, 2007, 19, 6518-6527.	6.7	52
44	Plasmon-Enhanced Layered Double Hydroxide Composite BiVO <sub>4</sub> Photoanodes: Layering-Dependent Modulation of the Water-Oxidation Reaction. ACS Applied Energy Materials, 2018, 1, 3577-3586.	5.1	52
45	Novel carbon nanostructures of caterpillar-like fibers and interwoven spheres with excellent surface super-hydrophobicity produced by chemical vapor deposition. Journal of Materials Chemistry, 2008, 18, 1245.	6.7	50
46	Co–Al mixed metal oxides/carbon nanotubes nanocomposite prepared via a precursor route and enhanced catalytic property. Journal of Solid State Chemistry, 2013, 197, 14-22.	2.9	49
47	Fabricating roughened surfaces on halloysite nanotubes via alkali etching for deposition of high-efficiency Pt nanocatalysts. CrystEngComm, 2015, 17, 3110-3116.	2.6	49
48	Acidic Electrochemical Reduction of CO <sub>2</sub> Using Nickel Nitride on Multiwalled Carbon Nanotube as Selective Catalyst. ACS Sustainable Chemistry and Engineering, 2019, 7, 6106-6112.	6.7	49
49	Insights into the Multiple Synergies of Supports in the Selective Oxidation of Glycerol to Dihydroxyacetone: Layered Double Hydroxide Supported Au. ACS Catalysis, 2020, 10, 12437-12453.	11.2	48
50	Liquid-Phase Hydrogenation of Cinnamaldehyde: Enhancing Selectivity of Supported Gold Catalysts by Incorporation of Cerium into the Support. Industrial & Engineering Chemistry Research, 2013, 52, 288-296.	3.7	47
51	Roughening of windmill-shaped spinel Co <sub>3</sub> O <sub>4</sub> microcrystals grown on a flexible metal substrate by a facile surface treatment to enhance their performance in the oxidation of water. RSC Advances, 2014, 4, 43357-43365.	3.6	47
52	Highly Efficient Separation of Magnesium and Lithium and High-Valued Utilization of Magnesium from Salt Lake Brine by a Reaction-Coupled Separation Technology. Industrial & Engineering Chemistry Research, 2018, 57, 6618-6626.	3.7	47
53	The confined space electron transfer in phosphotungstate intercalated ZnAl-LDHs enhances its photocatalytic performance for oxidation/extraction desulfurization of model oil in air. Green Chemistry, 2018, 20, 5509-5519.	9.0	47
54	Carbon-supported high-entropy Co-Zn-Cd-Cu-Mn sulfide nanoarrays promise high-performance overall water splitting. Nano Research, 2022, 15, 6054-6061.	10.4	47

#	Article	IF	CITATIONS
55	Recycling-oriented cathode materials design for lithium-ion batteries: Elegant structures versus complicated compositions. Energy Storage Materials, 2021, 41, 380-394.	18.0	46
56	Mediating the Oxidizing Capability of Surface-Bound Hydroxyl Radicals Produced by Photoelectrochemical Water Oxidation to Convert Glycerol into Dihydroxyacetone. ACS Catalysis, 2022, 12, 6946-6957.	11.2	45
57	Ni-based supported catalysts from layered double hydroxides: Tunable microstructure and controlled property for the synthesis of carbon nanotubes. Chemical Engineering Journal, 2009, 155, 474-482.	12.7	44
58	Polymeric carbon nitride with frustrated Lewis pair sites for enhanced photofixation of nitrogen. Journal of Materials Chemistry A, 2020, 8, 13292-13298.	10.3	44
59	Effect of Mo doping and NiFe-LDH cocatalyst on PEC water oxidation efficiency. Journal of Colloid and Interface Science, 2019, 540, 9-19.	9.4	43
60	Enhanced Activity of Supported Ni Catalysts Promoted by Pt for Rapid Reduction of Aromatic Nitro Compounds. Nanomaterials, 2016, 6, 103.	4.1	40
61	Ag/Ultrathin-Layered Double Hydroxide Nanosheets Induced by a Self-Redox Strategy for Highly Selective CO <sub>2</sub> Reduction. ACS Applied Materials & Interfaces, 2021, 13, 16536-16544.	8.0	40
62	Uniform CdS-decorated carbon microsheets with enhanced photocatalytic hydrogen evolution under visible-light irradiation. Journal of Alloys and Compounds, 2019, 770, 886-895.	5.5	39
63	Highly Efficient Lithium Extraction from Brine with a High Sodium Content by Adsorption-Coupled Electrochemical Technology. ACS Sustainable Chemistry and Engineering, 2021, 9, 11022-11031.	6.7	38
64	Highly Active Supported Pt Nanocatalysts Synthesized by Alcohol Reduction towards Hydrogenation of Cinnamaldehyde: Synergy of Metal Valence and Hydroxyl Groups. Chemistry - an Asian Journal, 2015, 10, 1561-1570.	3.3	37
65	One-dimensional gallium nitride micro/nanostructures synthesized by a space-confined growth technique. Applied Physics A: Materials Science and Processing, 2007, 87, 651-659.	2.3	35
66	Investigation of the structure and surface characteristics of Cu–Ni–M(III) mixed oxides (M=Al, Cr and) Tj ETQ	0q0_0 0 rgl 6.1 0 rgl	3T JOverlock
67	Determination of boundary conditions for highly efficient separation of magnesium and lithium from salt lake brine by reaction-coupled separation technology. Separation and Purification Technology, 2019, 229, 115813.	7.9	34
68	Enhancing Light-Driven Production of Hydrogen Peroxide by Anchoring Au onto C3N4 Catalysts. Catalysts, 2018, 8, 147.	3.5	33
69	Ni <sup>0</sup> /Ni <sup>δ+</sup> Synergistic Catalysis on a Nanosized Ni Surface for Simultaneous Formation of C–C and C–N Bonds. ACS Catalysis, 2019, 9, 11438-11446.	11.2	32
70	Acid–Base Promoted Dehydrogenation Coupling of Ethanol on Supported Ag Particles. Industrial & Engineering Chemistry Research, 2020, 59, 3342-3350.	3.7	31
71	A Facile and Green Synthesis Route to Mesoporous Spinel-type Znâ^'Al Complex Oxide. Industrial & Engineering Chemistry Research, 2008, 47, 1495-1500.	3.7	27
72	Formation and catalytic performance of supported ni nanoparticles via selfâ€reduction of hybrid NiAl‣DH/C composites. AICHE Journal, 2010, 56, 2934-2945.	3.6	26

#	Article	IF	CITATIONS
73	Template-assisted fabrication of macroporous NiFe2O4 films with tunable microstructural, magnetic and interfacial properties. Journal of Materials Chemistry, 2010, 20, 7378.	6.7	26
74	Controlling the Structure and Photoelectrochemical Performance of BiVO4 Photoanodes Prepared from Electrodeposited Bismuth Precursors: Effect of Zinc Ions as Directing Agent. Industrial & Engineering Chemistry Research, 2015, 54, 10723-10730.	3.7	24
75	Transition Metal Substitution Effects on Metal-to-Polyoxometalate Charge Transfer. Inorganic Chemistry, 2016, 55, 4308-4319.	4.0	24
76	Preparation of LiOH through BMED process from lithium-containing solutions: Effects of coexisting ions and competition between Na+ and Li+. Desalination, 2021, 512, 115126.	8.2	24
77	Doping of Chlorine from a Neoprene Adhesive Enhances Degradation Efficiency of Dyes by Structured TiO2-Coated Photocatalytic Fabrics. Catalysts, 2020, 10, 69.	3.5	24
78	Hydrophilic Modification Using Polydopamine on Core–Shell Li <sub>1.6</sub> Mn <sub>1.6</sub> O <sub>4</sub> @Carbon Electrodes for Lithium Extraction from Lake Brine. ACS Sustainable Chemistry and Engineering, 2022, 10, 8970-8979.	6.7	22
79	Porous and superparamagnetic magnesium ferrite film fabricated via a precursor route. Journal of Alloys and Compounds, 2010, 499, 30-34.	5.5	20
80	Pd-Co2P nanoparticles supported on N-doped biomass-based carbon microsheet with excellent catalytic performance for hydrogen evolution from formic acid. Applied Surface Science, 2020, 530, 147191.	6.1	20
81	Highly Efficient Lithium Recovery from Pre-Synthesized Chlorine-Ion-Intercalated LiAl-Layered Double Hydroxides via a Mild Solution Chemistry Process. Materials, 2019, 12, 1968.	2.9	19
82	Thermo-responsive polymer grafted carbon nanotubes as the catalyst support for selective hydrogenation of cinnamaldehyde: Effects of surface chemistry on catalytic performance. Applied Catalysis A: General, 2019, 575, 11-19.	4.3	19
83	Recent Advances in Layered Double Hydroxide-Based Materials as Versatile Photocatalysts. Reviews in Advanced Sciences and Engineering, 2014, 3, 158-171.	0.6	19
84	Hybrid ZnAl‣DH/CNTs nanocomposites: Noncovalent assembly and enhanced photodegradation performance. AICHE Journal, 2010, 56, 768-778.	3.6	18
85	Photo-responsive behaviors and structural evolution of carbon-nanotube-supported energetic materials under a photoflash. Materials Letters, 2012, 88, 27-29.	2.6	18
86	Enhanced Hydrogen Production from Ethanol Photoreforming by Site-Specific Deposition of Au on Cu2O/TiO2 p-n Junction. Catalysts, 2020, 10, 539.	3.5	18
87	Atomic Pt-Catalyzed Heterogeneous Anti-Markovnikov C–N Formation: Pt <sub>1</sub> <sup>0</sup> Activating N–H for Pt <sub>1</sub> <sup>Î′+</sup> -Activated Câ•C Attack. Journal of the American Chemical Society, 2020, 142, 9017-9027.	13.7	18
88	A nanocomposite precursor strategy to mixed-metal oxides with excellent catalytic activity for thermal decomposition of ammonium perchlorate. Applied Clay Science, 2012, 65-66, 14-20.	5.2	17
89	Atomic Ru catalysis for ethanol coupling to C4+ alcohols. Applied Catalysis B: Environmental, 2022, 309, 121271.	20.2	17
90	Construction of interconnected NiO/CoFe alloy nanosheets for overall water splitting. Renewable Energy, 2022, 194, 459-468.	8.9	15

#	Article	IF	CITATIONS
91	Ultrafine Co <sub>3</sub> O <sub>4</sub> nanolayer-shelled CoWP nanowire array: a bifunctional electrocatalyst for overall water splitting. RSC Advances, 2020, 10, 29326-29335.	3.6	14
92	Z-Scheme ZnM-LDHs/g-C <sub>3</sub> N <sub>4</sub> (M = Al, Cr) Photocatalysts: Their Desulfurization Performance and Mechanism for Model Oil with Air. Energy & Fuels, 2020, 34, 14676-14687.	5.1	13
93	Insights into Photocatalytic Selective Dehydrogenation of Ethanol over Au/Anatase–Rutile TiO <sub>2</sub> . Industrial & Engineering Chemistry Research, 2021, 60, 12282-12291.	3.7	11
94	Selective Photocatalytic Activation of Ethanol C–H and O–H Bonds over Multi-Au@SiO <sub>2</sub> /TiO <sub>2</sub> : Role of Catalyst Surface Structure and Reaction Kinetics. ACS Applied Materials & Interfaces, 2022, 14, 2848-2859.	8.0	10
95	Synthesis of poly(AAâ€ <i>co</i> â€AM) superabsorbent composites by reinforcement of halloysite nanotubes. Polymer Composites, 2015, 36, 229-236.	4.6	7
96	CoGa Particles Stabilized by the Combination of Alloyed Ga <sup>0</sup> and Lattice Ga <sup>III</sup> Species. Industrial & Engineering Chemistry Research, 2020, 59, 8649-8660.	3.7	6
97	Interfacial Sites in Ag Supported Layered Double Oxide for Dehydrogenation Coupling of Ethanol to <i>n</i> â€Butanol. ChemistryOpen, 2021, 10, 1095-1103.	1.9	5
98	Synthesis of Tunable-Acidity Vanadium Phosphorus Oxide Catalysts Modified by Layered Double Oxide for the Selective Oxidation of <i>n</i> -Butane. Industrial & Engineering Chemistry Research, 2022, 61, 3850-3859.	3.7	5
99	Nucleation–Oxidation coupled technology for High-Nickel ternary cathode recycling of spent Lithium-ion batteries. Separation and Purification Technology, 2022, 298, 121569.	7.9	5
100	Novel 2D self-assembled arrays of SiOx nanowire bundles. Materials Letters, 2007, 61, 3662-3665.	2.6	4
101	Ternary Composite of Biomass Porous Carbon/SnO 2 /Pt: An Efficient Catalyst for Reduction of Aromatic Nitro Compounds. ChemistrySelect, 2018, 3, 5066-5072.	1.5	4
102	Effects of temperature on laser diode ignition. Optik, 2009, 120, 85-88.	2.9	3
103	Direct preparation of batteryâ€grade lithium carbonate via a nucleation–crystallization isolating process intensified by a microâ€liquid film reactor. Canadian Journal of Chemical Engineering, 2023, 101, 870-882.	1.7	3
104	INVESTIGATION ON OXYGEN-EQUILIBRIUM EFFECTS OF LASER IGNITION OF ENERGETIC MATERIALS. Modern Physics Letters B, 2006, 20, 353-358.	1.9	2
105	The preparation of PLL–GRGDS modified PTSG copolymer scaffolds and their effects on manufacturing artificial salivary gland. Journal of Biomaterials Science, Polymer Edition, 2013, 24, 1721-1739.	3.5	2
106	<italic>In-situ</italic> conversion and catalytic properties of mixed-metal oxide catalysts for photosynthesis of hydrogen peroxide. Scientia Sinica Chimica, 2017, 47, 465-473.	0.4	2
107	Liquid-Phase Synthesis of NiO-Loaded Ag Nanoparticles and Enhanced Photo-Degradation Performance. Advanced Materials Research, 0, 287-290, 145-149.	0.3	1
108	Hierarchical Structures of Silicon Oxynitride Nanowires Formed by a Gallium-Catalyzed <i>In Situ</i> Reactive Technique. Advanced Materials Research, 2011, 284-286, 717-721.	0.3	1

#	Article	IF	CITATIONS
109	Indium-substituted <font>ZnO</font> /reduced graphene oxide nanocomposites: Solvothermal synthesis and enhanced visible-light-driven photocatalytic activity. Functional Materials Letters, 2014, 07, 1450013.	1.2	1
110	Assessment on the Water Vapor Flux from Atmospheric Reanalysis Data in the South China Sea on 2019 Summer. Journal of Hydrometeorology, 2022, 23, 847-858.	1.9	1